

Serveur Académique Lausannois SERVAL serval.unil.ch

Author Manuscript

Faculty of Biology and Medicine Publication

This paper has been peer-reviewed but does not include the final publisher proof-corrections or journal pagination.

Published in final edited form as:

Title: A fluorescent hormone biosensor reveals the dynamics of jasmonate signalling in plants.

Authors: Larrieu A, Champion A, Legrand J, Lavenus J, Mast D, Brunoud G, Oh J, Guyomarc'h S, Pizot M, Farmer EE, Turnbull C, Vernoux T, Bennett MJ, Laplaze L

Journal: Nature communications

Year: 2015 Jan 16

Volume: 6

Pages: 6043

DOI: [10.1038/ncomms7043](https://doi.org/10.1038/ncomms7043)

In the absence of a copyright statement, users should assume that standard copyright protection applies, unless the article contains an explicit statement to the contrary. In case of doubt, contact the journal publisher to verify the copyright status of an article.

Published in final edited form as:

Nat Commun. ; 6: 6043. doi:10.1038/ncomms7043.

A fluorescent hormone biosensor reveals the dynamics of jasmonate signalling in plants

Antoine Larrieu^{#1,2}, Antony Champion^{#3,4}, Jonathan Legrand¹, Julien Lavenus³, David Mast¹, Géraldine Brunoud¹, Jaesung Oh^{2,8}, Soazig Guyomarc'h⁵, Maxime Pizot³, Edward E. Farmer⁶, Colin Turnbull⁷, Teva Vernoux^{#1}, Malcolm J. Bennett^{2,†}, and Laurent Laplace^{3,4,†,*}

¹Laboratoire de Reproduction et Développement des Plantes, CNRS, INRA, ENS Lyon, UCBL, Université de Lyon, 69364 Lyon, France ²Centre for Plant Integrative Biology, University of Nottingham, LE12 5RD, UK ³Institut de Recherche pour le Développement, Unité Mixte de Recherche Diversité Adaptation et Développement des plantes, 34394 Montpellier, France ⁴Laboratoire mixte international Adaptation des Plantes et microorganismes associés aux Stress Environnementaux, Dakar, Senegal ⁵Université Montpellier 2, Unité Mixte de Recherche Diversité Adaptation et Développement des plantes, 34394 Montpellier, France ⁶Department of Plant Molecular Biology, Université de Lausanne, Switzerland ⁷Department of Life Sciences, Imperial College London, London, SW7 2AZ, UK

These authors contributed equally to this work.

Abstract

Activated forms of jasmonic acid (JA) are central signals coordinating plant responses to stresses, yet tools to analyse their spatial and temporal distribution are lacking. Here we describe a JA perception biosensor termed Jas9-VENUS that allows the quantification of dynamic changes in JA distribution in response to stress with high spatiotemporal sensitivity. We show that Jas9-VENUS abundance is dependent on bioactive JA isoforms, the COI1 co-receptor, a functional Jas motif and proteasome activity. We demonstrate the utility of Jas9-VENUS to analyse responses to JA *in planta* at a cellular scale both quantitatively and dynamically. This included using Jas9-VENUS to determine the cotyledon-to-root JA signal velocities upon wounding, revealing two distinct phases of JA activity in the root. Our results demonstrate the value of developing quantitative sensors such as Jas9-VENUS to provide high-resolution spatiotemporal data about hormone distribution in response to plant abiotic and biotic stresses.

Users may view, print, copy, and download text and data-mine the content in such documents, for the purposes of academic research, subject always to the full Conditions of use:http://www.nature.com/authors/editorial_policies/license.html#terms

*Correspondence should be addressed to L.L. (laurent.laplace@ird.fr).

⁸Present address: Plasma Technology Research Center, National Fusion Research Institute, Gunsan-City, Republic of Korea

Author contributions

A.L., A.C., E.F., C.T., T.V., M.J.B. and L.L. designed the experiments; A.L., A.C., J.L., J.L., D.M., G.B., J.O., S.G., and M.P. performed the experiments; A.L., A.C., T.V., M.J.B., and L.L. wrote the manuscript; all the authors read and edited the final manuscript; T.V., M.J.B. and L.L. supervised the project.

[†]These authors contributed equally to this work

Competing financial interests

The authors declare no competing financial interests.

Introduction

Plants are subject to a variety of biotic and abiotic stresses such as the presence of pathogens, insect or mechanical injury, and several environmental stresses. These stresses lead to changes in hormone levels and gene expression that occur within minutes and activate local and systemic responses. Many of these adaptive responses are regulated by the plant hormone jasmonic acid and its derivatives, collectively referred to as jasmonates (JA)¹. However, due to the current lack of tools to visualize the sites of JA perception *in planta*, there are major gaps in our understanding of how JA exerts its effects locally or systemically. JA signalling triggers large-scale changes in gene expression². In cells with a low JA content transcription factors that regulate JA-responsive genes are repressed by members of the JASMONATE ZIM-DOMAIN (JAZ) protein family. The bioactive form of JA conjugated to isoleucine, termed JA-Ile, promotes the binding of JAZ repressors to the F-box protein CORONATINE INSENSITIVE1 (COI1). This F-box protein is part of the SCF^{COI1} E₃ ubiquitin ligase complex that promotes JAZ degradation via the ubiquitin/26S proteasome pathway. Therefore, in the presence of JA-Ile, JAZ proteins are degraded and transcription factors are relieved from repression^{3,4,5}. A specific Jas motif in JAZ protein is responsible for their interaction with COI1 and their JA-dependent degradation^{6,7}.

Biosensors are tools that transform a recognition event such as the perception of a small molecule by a receptor into a signal that can be easily detected and quantified^{8,9}. In theory, a biosensor should 1) respond specifically to its target, 2) demonstrate a quantitative response over a physiologically relevant concentration range, 3) provide a dynamic and spatially-resolved response *in vivo* and 4) have no impact on the endogenous signalling system it is reporting^{8,9}. The recent development of biosensors for phytohormones such as auxin or ABA has led to significant progress in our understanding of the distribution of these molecules and their signalling mechanisms^{10,11,12}. Here we describe a novel JA perception biosensor termed Jas9-Venus and demonstrate its utility to quantitatively and dynamically analyse JA response and distribution *in planta* at the cellular scale.

Results

Jas9-VENUS is a biosensor for perception of bioactive JA

Previous studies have shown that JAZ proteins such as JAI3 and JAZ1 are degraded by the proteasome pathway in response to JA and that this degradation is dependent on a specific Jas motif in the protein^{3,4}. This provided a potential mechanism to develop biosensors to follow JA perception *in vivo*. In order to test this hypothesis, we generated translational fusions between the putative Jas motif of AtJAZ1 and AtJAZ9 proteins, including key amino acid residues on either side of the Jas motif⁶, the fast maturing VENUS variant of the yellow fluorescent protein^{13,14} and a N7 Nuclear Localization Signal (¹⁵, Fig. 1a). The corresponding constructs were expressed under the control of the constitutive CaMV 35S promoter and transformed into *Arabidopsis thaliana* plants expressing a nuclear Histone H2B marker fused to the Red Fluorescent Protein (H2B-RFP), under the regulation of the same promoter, for ratiometric measurements¹⁶ (Supplementary Fig. 1a-c). This approach limits biases in fluorescence levels that would be due to altered regulation of the CaMV 35S promoter. Robust fluorescence was only observed for Jas^{JAZ9}-VENUS lines, suggesting that

Jas^{JAZ1}-VENUS turnover is faster than its maturation time. This is consistent with the fast turnover observed for a JAZ1-GUS fusion⁴. We therefore focused our studies on Jas^{JAZ9}-VENUS, henceforth called Jas9-VENUS.

Next, we probed the quantitative relationship between Jas9-VENUS and JAs. We analysed changes in fluorescence in transgenic seedlings following JA treatment using confocal microscopy. The bacterial toxin coronatine is structurally similar to JA-Ile and is a potent agonist of the JA receptor⁷. We observed that low levels of coronatine led to rapid degradation of Jas9-VENUS in plant roots (Fig. 1b,d, Supplementary Fig. 1d and Supplementary Movie 1). Time course imaging of roots revealed that the Jas9-VENUS signal started to decrease within minutes after coronatine treatments. Western blot analyses confirmed that the decrease in fluorescence was due to Jas9-VENUS degradation (Fig. 1c). Fluorescence quantification indicated that Jas9-VENUS degradation was dose-dependent (Fig. 1d) and specifically induced by bioactive JAs (Fig. 1e) but not, or very delayed and only to a limited degree, by other hormones such as auxin, abscisic acid (ABA), ethylene (ACC, ethylene precursor) or salicylic acid (SA) (Fig. 1f). The limited and delayed degradation of Jas9-VENUS observed upon treatment with other hormones is likely to result from crosstalk between these signals and their transduction pathways with JA signaling¹⁷. The JA-Ile precursors, JA and 12-oxo-phytodienoic acid (OPDA) triggered a very rapid response indicating that these molecules quickly enter the cell and get metabolized to generate JA-Ile (Fig. 1e). Moreover, degradation of Jas9-VENUS was abolished in the *coil-1* mutant background¹⁸ and strongly reduced when plants were treated with the proteasome inhibitor MG132 (Fig. 1g). A stabilized Jas9-VENUS version was created by site-directed mutagenesis on the critical amino acids R and K at position 223 and 224 of the Jas motif being substituted with alanine residues. These mutations have been demonstrated to prevent binding to COI1 and therefore JAZ proteins degradation in response to JA treatments¹⁹. This mutated version of the sensor, termed mJas9-VENUS, was not degraded in response to coronatine treatment (Fig. 1g). Altogether, these data indicate that Jas9-VENUS is a quantitative and specific sensor of jasmonate perception *in planta*.

Next, we compared the growth response of Jas9-VENUS and control (Pro35S:H2B-RFP) plants to coronatine. Dose-response curves revealed that Jas9-VENUS roots exhibit the same profile of root growth inhibition by coronatine as control plants (Supplementary Fig. 2a). Similarly, the induction of JA-responsive genes in response to wounding was maintained in Jas9-VENUS plants (Supplementary Fig. 2b). Hence, our data indicate that the Jas9-VENUS sensor has no detectable effect on either physiological or molecular responses to JA.

Use of Jas9-VENUS to map local changes in JA distribution

JA inhibits root growth, notably through the direct repression of *PLETHORA* (*PLT*) genes by the transcription factor MYC2²⁰. However, the spatial distribution of JA in the root meristem remains unclear. We used Jas9-VENUS and H2B-RFP fluorescence to generate a map of JA distribution in the root apical meristem (Fig. 2a, Supplementary Fig. 3 and Supplementary Data 1). Since Jas9-VENUS degradation is COI1-dependent, we first analysed the expression of *COI1* in the root using a translational Pro_{COI1}:COI1-VENUS

fusion. The construct revealed a homogenous distribution of the receptor in the majority of root cell types (Supplementary Fig. 4 and Supplementary Data 1). Slightly higher expression was detected in elongating epidermal cells and these cells might therefore be more sensitive to JA. However, the spatial pattern of Jas9-VENUS fluorescence that we observed in the root apical meristem should not be influenced by differences in JA perception except in the mature epidermis, where potential overestimation of JA levels occurs due to high expression of *COI1*. Our imaging studies revealed that basal JA levels are higher in the epidermal, ground tissue, pericycle and vascular initials and in their daughter cells in the division zone than in other parts of the root (Fig. 2a and Supplementary Fig. 3). Interestingly, a root JA gradient was revealed with highest concentrations close to the tip which decreased as cells move away from the stem cell niche. Low JA accumulation occurred in the quiescent centre. Considering that jasmonate is a stress-related hormone present at low concentrations in unstimulated tissues²¹, this suggests a role for JA in the functioning of the root apical meristem. No JA was found to accumulate in the root cap except in last two cells of the lateral root cap. Hence, Jas9-VENUS together with the *COI1* translational reporter can be used to map the distribution of JA in a given cell, tissue or organ.

Mechanical stress is also known to trigger JA production in plants²¹. We therefore investigated the dynamics of local response of the Jas9-VENUS sensor to mechanical stress by applying a mechanical pressure to roots using an agar block. The reporter was degraded in all of the cells under pressure in less than 20 minutes indicating that JA signalling was rapidly activated throughout the root (Fig. 2b). The degradation was again *COI1*-dependent as demonstrated by the lack of response in a *coi1-1* mutant background or in the mJas9-VENUS line (Fig. 2b). Similarly, perturbations in cell wall properties by genetic (mutations) or pharmacological (isoxaben) inhibition of cellulose biosynthesis lead to mechanical stress and JA production^{22,23}. Consistently, we observed a rapid degradation of the Jas9-VENUS sensor starting in the elongation zone around 110 min after isoxaben treatment and then moving to neighbouring regions of the root apex (Fig. 2c-e and Supplementary Movie 2). Hence, the Jas9-VENUS sensor reveals JA-Ile perception at a cellular resolution in plant roots in response to local stresses and allows the spread of the JA signal to be monitored at the tissue level.

Use of Jas9-VENUS to study long-distance JA signalling

The mechanisms by which plants perceive and respond to tissue injury are complex. Biotic or mechanical stresses lead to systemic induction of host defence responses that protects healthy tissues from secondary attack. This JA-mediated process involves long-distance communication between tissues²⁴ and occurs within minutes of tissue injury. In order to analyse long distance JA signalling, we measured VENUS fluorescence in the root following wounding of one cotyledon. We observed a rapid decrease in Jas9-VENUS fluorescence in the root (Fig 3a, Supplementary Fig. 5 and Supplementary Movie 3). In contrast to local mechanical stress, the decrease in VENUS fluorescence occurred in two distinct phases in 10 of 14 experiments (Fig 3a and Supplementary Fig. 5). An initial phase amounting to a loss of ~8% of the signal was completed ~2 minutes after wounding (Fig 3a). This first phase was mainly detected in the stele suggesting that the signal was moving in the vasculature (Fig 3a and Supplementary Fig. 5). In order to determine the velocity of the

signal triggered by wounding, fluorescence was measured at 4 different positions along the root (Fig 3b). Interestingly, the loss of VENUS fluorescence characteristic of this first phase occurred simultaneously at the root/shoot junction (Zone 1) and in close vicinity of the root tip (Zone 4), which were 1cm apart. Based on the experiment set-up, we estimate the speed of this first wave to exceed 1 cm min^{-1} . This observation is in the same order of magnitude as measurements reported for leaf to leaf wound signaling²⁵. A second phase observed in all experiments started at ~30 minutes and lasted for 90 minutes leading to a further 70% decrease of the fluorescence signal. It occurred first in the stele and then in the outer tissues and starts in the root tip region (Zone 4; Fig 3a and Supplementary Fig. 5). Using RT-qPCR we confirmed that the decrease in VENUS fluorescence after wounding was not due to an altered expression of the receptor *COII* and of the sensor *Jas9-VENUS* as the expression of both mRNA is stable after wounding in the shoot and in the root (Supplementary Fig. 6a,b). We also showed that the reduction in VENUS fluorescence in response to wounding required a functional Jas motif (Supplementary Fig. 7). Thus, the Jas9-VENUS reporter revealed that a two-step JA response is induced in the root in response to wounding in the aerial part of the plant and allows the estimation of the speed of the signal triggering this response.

We investigated whether the response observed with the Jas9-VENUS sensor could be correlated with documented JA responses. Roots and aerial parts from Arabidopsis plants were harvested before and 30 min and 2h after wounding a cotyledon and the expression of genes induced by JA was measured by RT-qPCR. We observed a rapid induction of JA-responsive genes in roots after wounding in accordance with the rapid response of the Jas9-VENUS reporter (Fig. 3c). This induction is dependent on JA production since the biosynthesis mutant *aos*²⁶ exhibited little or no induction of those genes (Fig. 3c). Moreover, JA was recently shown to stabilize the JA-responsive MYC2 transcription factor²⁷. Accordingly, we observed that a stabilization of a MYC2-GFP fusion protein in the root 1h after wounding the cotyledon (Supplementary Fig. 8). This stabilization was lost in a MYC2 DE-GFP construct that was shown to be unable to respond to JA²⁷. This is consistent with an induction of local JA production in the root corresponding to the second phase of the response detected with Jas9-VENUS. Altogether, gene expression data and MYC2 protein stabilization are consistent with the dynamics of JA signalling that we observed with the Jas9-VENUS sensor.

Discussion

Here we describe Jas9-VENUS, a new tool to monitor the perception of biologically active jasmonates *in planta*. We show that Jas9-VENUS is specifically and rapidly degraded in the presence of bioactive JA in a dose-dependent manner. Moreover, we demonstrate that Jas9-VENUS degradation is dependent on COII and the proteasome. Finally, our results indicate that the Jas9-VENUS construct does not perturb JA perception and responses. Altogether, Jas9-VENUS has all the attributes of a JA perception biosensor, i.e. its fluorescence is directly correlated to the combinatorial action of the signal and the receptor machinery.

Our results suggest that Jas9 might be more stable than other Jas motifs such as Jas1 and might therefore not be as responsive for fast JA responses or suitable to calculate velocity

for propagation of rapid JA responses. However, in practice Jas9-VENUS degradation was dose-dependent and responded very rapidly (in a few minutes) to JA. Moreover, analyses of JA-responsive gene expression are consistent with the observed dynamics of Jas9-VENUS degradation. Jas9-VENUS thus offers a good compromise between a strong fluorescence signal, sensitivity, specificity and a quantitative and rapid response, as expected from a genetically encoded-sensor⁹. In addition, we used of a ratiometric approach combining the Jas9-VENUS construct to a nuclear-localized 35S-H2B:RFP construct to prevent errors due to a transcriptional effect on the 35S promoter. However, we cannot rule out that the use of two different constructs containing the 35S promoter could still induce biases in ratio quantification due to genomic position effects that might impact the expression of the transgene or to silencing. Ideally, both Jas9-Venus and H2B-RFP would be expressed from the same promoter as a single protein that would be cleaved to avoid these problems²⁸. Such a design feature would prove useful in future biosensors development.

Our studies of local and long-distance JA responses showed the value of Jas9-VENUS to image the quantitative dynamics of these responses at a high temporal and spatial resolution. Using Jas9-VENUS we were able to generate a map of JA accumulation in the root apical meristem. Exogenous JA is known to regulate root growth¹ and jasmonates could mediate root response to various biotic and abiotic environmental signals. Here we show that JA accumulates in epidermis, ground tissues and vascular tissue from the initials to the end of the division zone in undamaged plants. This is coherent with the expression of the JA-inducible *ASA1* gene in the root tip²⁹. *ASA1* encodes an enzyme involved in auxin biosynthesis and this JA-auxin crosstalk could mediate some of the JA-regulated root responses to environmental signals. Moreover, our map revealed JA accumulation in the outer lateral root cap and in the epidermis. This is in agreement with previously reported map of JA-related gene expression in the root apical meristem³⁰, suggesting that JA distribution might be the primary determinant of JA-induced gene expression in this tissue. Interestingly, outer lateral root cap cells were shown to enter programmed cell death (PCD; ³¹). While the role of JA in PCD has been documented in other systems³², this suggests a novel role for JA in regulating lateral root cap development. Finally the high levels of JA detected in the ground tissue initials and daughter cells suggest an unanticipated role for JA in the activity of the root apical meristem.

We also used the Jas9-VENUS sensor to analyse long-distance signalling between the aerial parts and the root following a wound. It revealed that a two-step JA response is induced in the root in response to wounding in the aerial part of the plant. We first observed a rapid signal (>1 cm/min) moving through the stele and inducing a limited degradation of Jas9-VENUS presumably through a limited JA production. This first phase was relatively weak and localized in the stele but robust enough to be detected in 10 out of 14 experiments. Moreover, the variability of response we observed could also result from the difficulties of performing wounding in a reproducible way. In leaves, this fast moving signal is likely related to the membrane depolarization occurring in sieve elements in response to wounding and responsible for leaf-to-leaf signaling^{25,33}. A similar mechanism may participate in leaf-to-root signalling and might induce the very rapid conversion of a local pool of inactive jasmonate precursors into active JA. This would in turn trigger the expression of JA

biosynthesis genes and therefore strongly enhance JA accumulation that would contribute to the second phase of the response. This bi-phasic mechanism would therefore serve to amplify an initial rapid systemic signal to induce a later, stronger local response in the root. Electrical activity in the vasculature is probably not the only source of signals that lead to jasmonate production in wounded leaves²⁵ and it is possible that other mechanisms underlie the second, stronger phase of jasmonate signalling that we observed in roots. Importantly, our results suggest that wounding not only induces systemic defence in the leaves but is also likely to modulate root development, physiology and defence responses.

Jasmonate is a fundamental regulator of plant responses to various abiotic and biotic stresses. The Jas9-VENUS sensor paves the way to a better characterization of the JA signalling pathway *in planta*. Our results further illustrate how fluorescent sensors can be used to perform multi-scale analyses of the distribution of small signalling molecules.

Methods

Chemicals and hormones

Coronatine (COR), jasmonic acid (JA), salicylic acid (SA), α -naphthalene acetic acid (NAA), 1-aminocyclopropanecarboxylic acid (ACC, ethylene precursor), (\pm)-abscisic acid (ABA), MG132 and isoxaben were purchased from Sigma. 12-oxo phytyldienoic acid (OPDA) was purchased from Cayman chemical (Keystone, Colorado, USA). COR, SA, NAA, MG132 and isoxaben were dissolved in 100% dimethyl sulfoxide (DMSO), ACC was dissolved in ddH₂O, ABA in 100% methanol and JA in 100% ethanol. All compounds were dissolved to a stock concentration of 50 or 100 mM. OPDA was purchased diluted in 100% ethanol (100 μ g/100 μ l ~ 3.4mM).

Arabidopsis lines

The JA biosynthetic mutant *aos*²⁶ and the JA response mutant *coi1-1*¹⁸ were obtained from the Nottingham Arabidopsis Centre. The p35S:H2B-RFP, p35S:MYC2-GFP and p35S:MYC2 DE-GFP line were described previously^{16,27}.

Seed sterilization and plant growth

Seeds were surface sterilized for 5 minutes in 10 % bleach, 0.1 % triton X-100 then washed three times with sterile ddH₂O. Seeds were stratified at 4° for 2 days to synchronize germination. For time lapse imaging on the confocal microscope (treatments and wound responses) sterile seeds were sown directly onto glass bottom petri dishes (ref 627861 from Greiner (Germany), and ref 3930-035 from Iwaki (Japan)) against a block of 1/2 MS medium (2.17 g MS salts L⁻¹ (Sigma)) at pH 5.7 solidified with 1 % bacto-agar (Appleton Woods) (as shown on Supplementary Fig. 9). Seedlings were grown under continuous light (100 μ E m⁻² s⁻¹). For all other experiments (mechanical stress, bulk up, gene expression) sterile seeds were sown onto round or square petri dishes containing MS-agar media as described above.

Jas9-VENUS constructs

The Jas motif from *AtJAZ9* was amplified using primer JAZ9-F2 and JAZ9-R1 by PCR using cDNA produced from 2 weeks-old *Arabidopsis* plants treated with 50 μ M JA during 1 hour. The mutated version of the Jas9-VENUS sensor was generated by PCR using primers JAZ9-F3m and JAZ9-R3m. PCR products were cloned into pENTR-D TOPO (Invitrogen). The Jas motif sequence or the mutated version were then fused in-frame to VENUS-N7 under the control of the cauliflower mosaic virus 35S promoter in the pH7m34GW binary plasmid³⁴ using the Multisite Gateway three-fragment vector construction kit (Invitrogen). Plasmid constructs were confirmed by sequencing. The vectors were transformed into *Agrobacterium tumefaciens* strain GV3101 and into *Arabidopsis* p35S-H2B:RFP (Col-0 ecotype) using the floral dip transformation protocol. Lines with single insertions were selected based on the segregation of antibiotic resistance and fluorescence. Line # 6 was used in most experiments unless specifically stated.

COI1 constructs

COI1 genomic sequence and its promoter were amplified by PCR using COI1-Fw and COI1-Rev-Full primers. The PCR product was purified and cloned into the entry clone pENTR-D-TOPO using TOPO cloning (Invitrogen) according to the manufacturer's instructions. The fast maturing yellow fluorescent protein VENUS was added immediately before the STOP codon using multi-site gateway cloning into the destination vector pK7m34GW to create the binary vector pK7m34GWpCOI1-COI1-VENUS. The vector was transformed into *Agrobacterium* strain GV3101 and into *Arabidopsis* Col-0 ecotype using the floral dip transformation protocol³⁵.

Arabidopsis protein extraction

Extraction of soluble proteins was performed on 1 week old seedlings grown on 1/2 MS + agar plates. Seedlings were treated continuously with liquid 1/2 MS liquid medium for 30 minutes with 1 μ M coronatine or with DMSO (Mock). Seedlings were harvested, frozen in liquid nitrogen and then ground using a Qiagen Tissue Lyser II (30Hz during 30 seconds). The powder was resuspended in SDG buffer (0.0625 M Tris-HCl pH6.8; 2.5% SDS; 2% DTT (0.13M); 20% glycerol) and subjected to 3 cycles of freezing/thawing in liquid nitrogen. Proteins were boiled for 5 minutes at 95°C followed by two successive rounds of centrifugation (20 minutes, 18,000g at 4°C then 5 minutes, 18,000g at 4°C) to remove cell debris.

Western Blot

The samples were boiled for 5 minutes at 95°C before being loaded onto a gel (10 μ L per lane). SDS-PAGE was performed on 10% polyacrylamide gel. After transfer onto a nitrocellulose membrane protein amounts in each lane were checked using Ponceau staining. Immunoblotting analysis was realized using a primary rabbit polyclonal anti-GFP antibody (ab290, abcam, diluted 1:5000) and a secondary anti-rabbit Ig-HRP (NA934-1ML, Amersham, diluted 1:10000). Proteins were visualized using the Enhanced chemiluminescence kit (ECL, Amersham).

Confocal microscopy

Jas9-VENUS seedlings were imaged on an inverted Leica SP5 confocal laser scanning microscope (Leica Microsystems, Germany) or an inverted Nikon Eclipse Ti-U confocal microscope (Nikon, Japan). Scanner and detectors settings used for one experiment were optimized to avoid saturation and to maximize resolution and kept unchanged throughout the experiment. VENUS was excited using the 514nm line (Leica SP5) or the 488nm line (Nikon Eclipse) of an argon laser. VENUS fluorescence was collected from 520 to 560 nm (using the AOBS of the SP5) or using a 515/30 detector (Nikon Eclipse). RFP was excited using a 561 nm laser diode (SP5) or the 543nm line of a Green He/Ne laser (Nikon Eclipse). RFP fluorescence was collected from 590 to 680 nm (using the AOBS of the SP5) or using a 605/75 detector (Nikon Eclipse).

Images were taken with a fixed delay of 2 minutes over a minimum time of 1 hour using the 10x objective in order to maximize the number of nuclei being observed. Initially, seedlings were imaged following the protocol described¹⁶. Briefly, seedlings were grown onto 1/2 MS-agar round or square petri dishes and gently transferred onto glass bottom petri dishes. A small block of 1/2 MS-agar was slowly dropped onto the seedling and fluorescence was followed over time just above the elongation zone of the root. Initial experiments showed that such treatment induced the degradation of the Jas9-VENUS reporter. Subsequently, seeds were directly germinated onto the glass bottom petri dishes (as shown on Supplementary Fig.9) and roots that grew in between the agar block and the glass bottom were imaged. In such configuration a stable VENUS fluorescence could be followed over time in the absence of treatments, although the signal fluctuated over time (+/- 20%). Treatments were provided by adding liquid 1/2 MS solution (+ indicated chemicals) at the same temperature next to the seedling that was going to be imaged. Mock treatments resulted in no major changes in fluorescence (comparable to no addition of liquid medium).

Other markers (pCOI1:COI1-VENUS, p35S:MYC2-GFP and p35S:MYC2 DE-GFP) and images for the JA and COI1 root maps were imaged on an inverted Zeiss 710 confocal laser scanning microscope. Scanner and detectors settings used for one experiment were optimized to avoid saturation and to maximize resolution and kept unchanged throughout the experiment. VENUS was excited using the 514nm line of an argon laser and collected from 520 to 560 nm. GFP was excited using a 488 nm line of an argon laser and collected from 495 to 550 nm.

Fluorescence quantification

Fluorescence quantification was performed as described³⁶. Briefly, background fluorescence was removed using a threshold and only fluorescence coming from the nuclei was quantified. Plots presented show changes in raw integrated density values over time, measured using FIJI software. Ratios (raw integrated density of the VENUS channel divided by the raw integrated density of the red channel) were calculated using Microsoft Excel software.

JA and COI1 root maps

The acquired confocal images were imported for processing using Python programming language. Images with the lowest saturation possible were used to avoid computational artefacts and to preserve a good signal to noise ratio. Background (shown in white) was removed for the JA root maps by thresholding the H2B-RFP fluorescence to an intensity above 34 and for the COI1 root map by thresholding the COI1-VENUS fluorescence to an intensity above 16. For the JA root map, the ratiometric computation is the ratio of Jas9-VENUS/H2B-RFP fluorescence. To enhance the “high JA” and “low JA” differences, the obtained ratiometric values were transformed into a \log_{10} scale. For the COI1 root map, the COI1-VENUS fluorescence values were centred around the mean to enhance for differences in fluorescence.

RT qPCR

1-week old seedlings were wounded by cutting a cotyledon. RNA was extracted from shoots and root separately using the Spectrum Plant Total RNA kit (Sigma). Poly(dT) cDNA was prepared from 1 μ g of total RNA with Superscript III reverse transcriptase (Invitrogen) and analysed on a StepOnePlus apparatus (Life Technologies) with the SYBR® Green PCR Master Mix (Applied Biosystem) according to the manufacturer’s instructions. Targets genes were quantified with specific primer pairs designed with the Universal Probe Library Assay Design Center (Roche Applied Science). All reactions were done in quadruplicate and data were analysed with Microsoft Excel 2007 (Microsoft Corporation, Redmond, USA). Expression levels were normalised to At1G04850 (CTRL1) and calibrated to unwounded seedling using the Ct method.

Supplementary Material

Refer to Web version on PubMed Central for supplementary material.

Acknowledgements

We thank Pr. C. Li (Chinese Academy of Science) for kindly providing the 35S:MYC2-GFP-12 seeds and Dr. Tara Holman for the CTRL1 primer sequence. We acknowledge the support of the Région Languedoc-Roussillon (“Chercheur d’Avenir” grant to SG and LL), a Pludisciplinary Research Grant from the Université Montpellier 2 (SG and LL), the Agropolis Fondation “Rhizopolis” Federative Grant (JL, SG and LL) and Agence National de la Recherche grant ANR-12-BSV6-0005 grant (AL and TV). A.L. and M.J.B. acknowledge the support of the Biotechnology and Biological Sciences Research Council and Engineering and Physical Sciences Research Council funding to the Centre for Plant Integrative Biology. We also acknowledge funding in the form of a Biotechnology and Biological Sciences Research Council Professorial Research Fellowship (to M.J.B.) as well as funding in the form of a Biotechnology and Biological Sciences Research Council grant (A.L. and M.J.B.).

References

1. Wasternack C, Hause B. Jasmonates: biosynthesis, perception, signal transduction and action in plant stress response, growth and development. An update to the 2007 review in *Annals of Botany*. *Ann. Bot.* 2013; 111:1021–1058. [PubMed: 23558912]
2. Pauwels L, Inzé D, Goossens A. Jasmonate-inducible gene: What does it mean? *Trends PlantSci.* 2009; 14:87–91.
3. Chini A, et al. The JAZ family of repressors is the missing link in jasmonate signalling. *Nature*. 2007; 448:666–671. [PubMed: 17637675]

4. Thines B, et al. JAZ repressor proteins are targets of the SCFCO11 complex during jasmonate signalling. *Nature*. 2007; 448:661–665. [PubMed: 17637677]
5. Pauwels L, Goossens A. The JAZ Proteins: A Crucial Interface in the Jasmonate Signaling Cascade. *Plant Cell Online*. 2011; 23:3089–3100.
6. Sheard LB, et al. Jasmonate perception by inositol-phosphate-potentiated CO11-JAZ co-receptor. *Nature*. 2010; 468:400–405. [PubMed: 20927106]
7. Yan J, et al. The Arabidopsis CORONATINE INSENSITIVE1 Protein Is a Jasmonate Receptor. *Plant Cell Online*. 2009; 21:2220–2236.
8. Wells DM, Laplaze L, Bennett MJ, Vernoux T. Biosensors for phytohormone quantification: challenges, solutions, and opportunities. *Trends Plant Sci*. 2013; 18:244–249. [PubMed: 23291242]
9. Sadanandom A, Napier RM. Biosensors in plants. *Curr. Opin. Plant Biol*. 2010; 13:736–743. [PubMed: 20870451]
10. Brunoud G, et al. A novel sensor to map auxin response and distribution at high spatio-temporal resolution. *Nature*. 2012; 482:103–106. [PubMed: 22246322]
11. Jones AM, et al. Abscisic acid dynamics in roots detected with genetically encoded FRET sensors. *eLife*. 2014; 3:e01741. [PubMed: 24737862]
12. Waadt R, et al. FRET-based reporters for the direct visualization of abscisic acid concentration changes and distribution in Arabidopsis. *eLife*. 2014; 3:e01739. [PubMed: 24737861]
13. Shaner NC, Steinbach PA, Tsien RY. A guide to choosing fluorescent proteins. *Nat. Methods*. 2005; 2:905–909. [PubMed: 16299475]
14. Nagai T, et al. A variant of yellow fluorescent protein with fast and efficient maturation for cell-biological applications. *Nat. Biotechnol*. 2002; 20:87–90. [PubMed: 11753368]
15. Cutler SR, Ehrhardt DW, Griffiths JS, Somerville CR. Random GFP::cDNA fusions enable visualization of subcellular structures in cells of Arabidopsis at a high frequency. *Proc. Natl. Acad. Sci. U. S. A*. 2000; 97:3718–3723. [PubMed: 10737809]
16. Federici F, Dupuy L, Laplaze L, Heisler M, Haseloff J. Integrated genetic and computation methods for in planta cytometry. *Nat. Methods*. 2012; 9:483–485. [PubMed: 22466793]
17. Song S, Qi T, Wasternack C, Xie D. Jasmonate signaling and crosstalk with gibberellin and ethylene. *Curr. Opin. Plant Biol*. 2014; 21C:112–119. [PubMed: 25064075]
18. Xie D-X, Feys BF, James S, Nieto-Rostro M, Turner JG. CO11: An Arabidopsis Gene Required for Jasmonate-Regulated Defense and Fertility. *Science*. 1998; 280:1091–1094. [PubMed: 9582125]
19. Melotto M, et al. A critical role of two positively charged amino acids in the Jas motif of Arabidopsis JAZ proteins in mediating coronatine- and jasmonoyl isoleucine-dependent interactions with the CO11 F-box protein. *Plant J. Cell Mol. Biol*. 2008; 55:979–988.
20. Chen Q, et al. The basic helix-loop-helix transcription factor MYC2 directly represses PLETHORA expression during jasmonate-mediated modulation of the root stem cell niche in Arabidopsis. *Plant Cell*. 2011; 23:3335–3352. [PubMed: 21954460]
21. Glauser G, et al. Spatial and Temporal Dynamics of Jasmonate Synthesis and Accumulation in Arabidopsis in Response to Wounding. *J. Biol. Chem*. 2008; 283:16400–16407. [PubMed: 18400744]
22. Ellis C, Karafyllidis I, Wasternack C, Turner JG. The Arabidopsis mutant cev1 links cell wall signaling to jasmonate and ethylene responses. *Plant Cell*. 2002; 14:1557–1566. [PubMed: 12119374]
23. Desprez T, et al. Resistance against herbicide isoxaben and cellulose deficiency caused by distinct mutations in same cellulose synthase isoform CESA6. *Plant Physiol*. 2002; 128:482–490. [PubMed: 11842152]
24. Prime-A-Plant Group. et al. Priming: getting ready for battle. *Mol. Plant-Microbe Interact. MPMI*. 2006; 19:1062–1071. [PubMed: 17022170]
25. Mousavi SAR, Chauvin A, Pascaud F, Kellenberger S, Farmer EE. GLUTAMATE RECEPTOR-LIKE genes mediate leaf-to-leaf wound signalling. *Nature*. 2013; 500:422–426. [PubMed: 23969459]

26. Park J-H, et al. A knock-out mutation in allene oxide synthase results in male sterility and defective wound signal transduction in *Arabidopsis* due to a block in jasmonic acid biosynthesis. *Plant J. Cell Mol. Biol.* 2002; 31:1–12.
27. Zhai Q, et al. Phosphorylation-coupled proteolysis of the transcription factor MYC2 is important for jasmonate-signaled plant immunity. *PLoS Genet.* 2013; 9:e1003422. [PubMed: 23593022]
28. Wend S, et al. A quantitative ratiometric sensor for time-resolved analysis of auxin dynamics. *Sci. Rep.* 2013; 3:2052. [PubMed: 23787479]
29. Sun J, et al. *Arabidopsis* ASA1 is important for jasmonate-mediated regulation of auxin biosynthesis and transport during lateral root formation. *Plant Cell.* 2009; 21:1495–1511. [PubMed: 19435934]
30. Birnbaum K, et al. A gene expression map of the *Arabidopsis* root. *Science.* 2003; 302:1956–1960. [PubMed: 14671301]
31. Fendrych M, et al. Programmed cell death controlled by ANAC033/SOMBRERO determines root cap organ size in *Arabidopsis*. *Curr. Biol. CB.* 2014; 24:931–940. [PubMed: 24726156]
32. Reinbothe C, Springer A, Samol I, Reinbothe S. Plant oxylipins: role of jasmonic acid during programmed cell death, defence and leaf senescence. *FEBS J.* 2009; 276:4666–4681. [PubMed: 19663906]
33. Salvador-Recatalá V, Tjallingii WF, Farmer EE. Real-time, in vivo intracellular recordings of caterpillar-induced depolarization waves in sieve elements using aphid electrodes. *New Phytol.* 2014; 203:674–684. [PubMed: 24716546]
34. Karimi M, Bleys A, Vanderhaeghen R, Hilson P. Building Blocks for Plant Gene Assembly. *Plant Physiol.* 2007; 145:1183–1191. [PubMed: 17965171]
35. Clough SJ, Bent AF. Floral dip: a simplified method for *Agrobacterium*-mediated transformation of *Arabidopsis thaliana*. *Plant J. Cell Mol. Biol.* 1998; 16:735–743.
36. Larrieu AP, French AP, Pridmore TP, Bennett MJ, Wells DM. Time-profiling fluorescent reporters in the *Arabidopsis* root. *Methods Mol. Biol. Clifton NJ.* 2014; 1056:11–17.

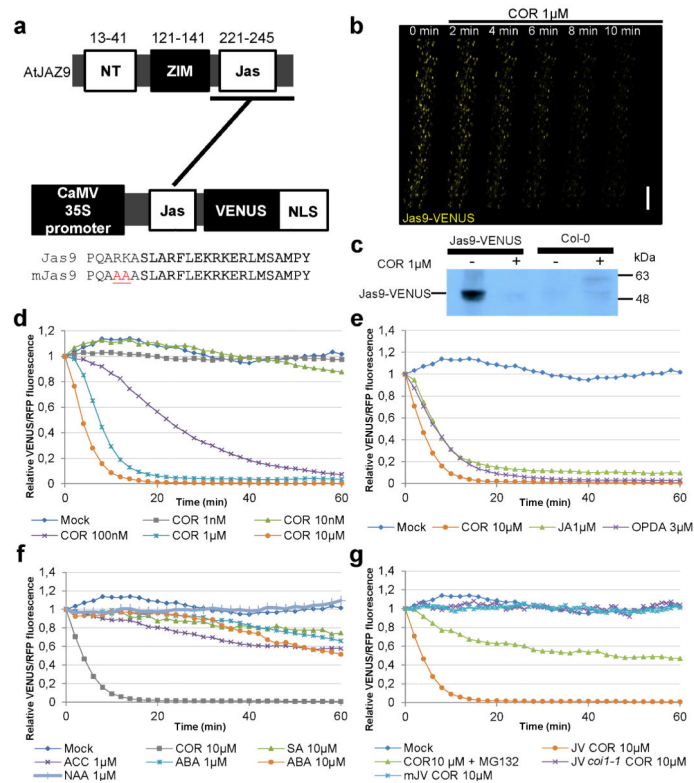


Figure 1. Jas9-VENUS is a biosensor for bioactive JA perception

(a) Schematic representation of the *AtJAZ9* gene, the Jas9-VENUS and mJas9-VENUS constructs, as well as the protein sequences of their respective Jas motif (NT: N Terminus, ZIM: ZIM motif, Jas: Jas motif, NLS: Nuclear Localization Signal). Numbers above the schematic represent amino acid position. (b) Time course confocal laser scanning micrographs of Jas9-VENUS at the indicated time points after treatments with 1 μ M coronatine (COR; scale bar = 100 μ m). (c) Western blot analysis of total protein extracts of Jas9-VENUS and Col-0 seedlings treated for 30 minutes with or without 1 μ M coronatine and probed with an anti-GFP antibody (uncropped western blot is shown in Supplementary Fig. 1d). (d) Time course quantification of Jas9-VENUS fluorescence, normalised to H2B-RFP fluorescence, in response to various concentrations of coronatine (n=3). (e) Time course quantification of Jas9-VENUS fluorescence, normalised to H2B-RFP fluorescence, in response to JA-Ile precursors jasmonic acid (JA) and 12-oxo-phytodienoic acid (OPDA) (n=2). (f) Time course quantification of Jas9-VENUS fluorescence, normalised to H2B-RFP fluorescence, in response to auxin (α -Naphthalene acetic acid (NAA)), abscisic acid (ABA), 1-Aminocyclopropanecarboxylic acid (ACC, ethylene precursor) or salicylic acid (SA) (n=2). (g) Time course quantification of Jas9-VENUS fluorescence, normalised to H2B-RFP fluorescence, in response to treatments with coronatine in a WT or a *coil-1* mutant, in response to coronatine and MG132 (proteasome inhibitor) treatments and of mJas9-VENUS fluorescence, normalised to H2B-RFP fluorescence, in response to coronatine (n=2). All the data shown derive from a representative experiments and the number of replications of each experiment is indicated. JV: Jas9-VENUS, mJV: mJas9-VENUS.

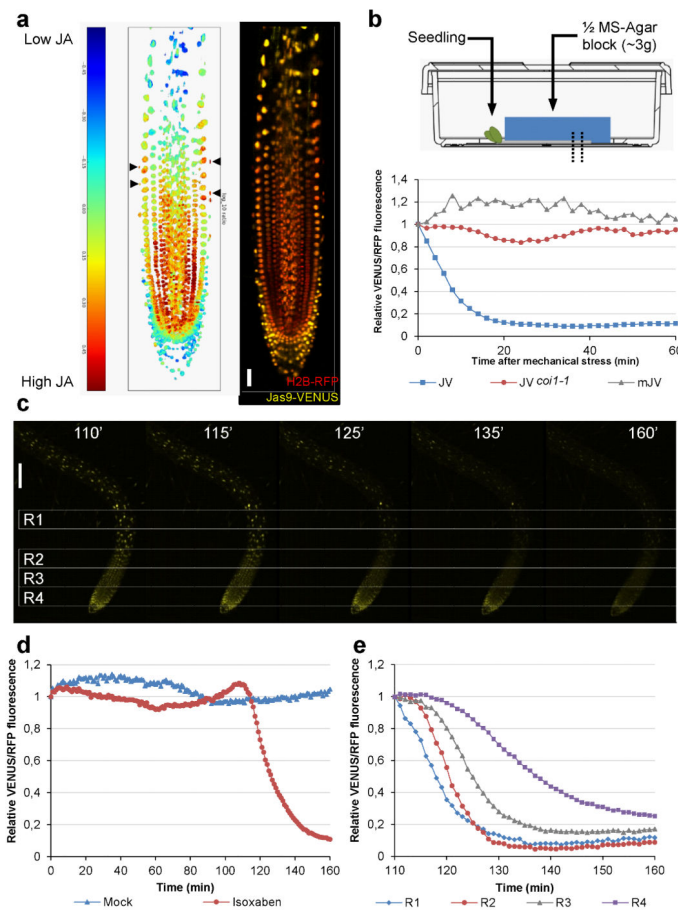


Figure 2. Jas9-VENUS can be used to map local changes in bioactive JA

(a) Distribution map of bioactive JA in the root apical meristem based on the ratio of Jas9-VENUS fluorescence to H2B-RFP fluorescence of a representative seedling. The overlay of the Jas9-VENUS and H2B-RFP channels used for generating the root map is shown (scale = 30 μ m). In total, 3 independent transgenic lines were analysed (n=5) and representative maps are shown in Supplementary Fig. 3. The map revealed that basal JA levels are higher in the epidermal, ground tissue, pericycle and vascular initials and in their daughter cells in the division zone than in other parts of the root. (b) Seedlings are mechanically stimulated by gently laying down a block of agar (~3g) on the entire root. Time course quantification of Jas9-VENUS fluorescence, normalised to H2B-RFP fluorescence, in a WT or *coi1-1* mutants and of mJas9-VENUS fluorescence, normalised to H2B-RFP fluorescence, in response to a mechanical stimulus. (c) Confocal micrographs taken at the indicated time points after treatments with 10 μ M isoxaben (scale bar = 100 μ m, n=2). (d) Time course quantification of Jas9-VENUS fluorescence, normalised to H2B-RFP fluorescence, over 160 minutes after isoxaben and mock treatments. (e) Time course quantification of Jas9-VENUS fluorescence, normalised to H2B-RFP fluorescence, between 110 and 160 minutes after treatments with isoxaben for the four regions of the root indicated on the micrographs. Drawing used in (b) kindly provided by Greiner Bio-One GmbH, Frickenhausen, Germany. All the data shown derive from a representative experiments and the number of replications of each experiment is indicated. JV: Jas9-VENUS, mJV: mJas9-VENUS.

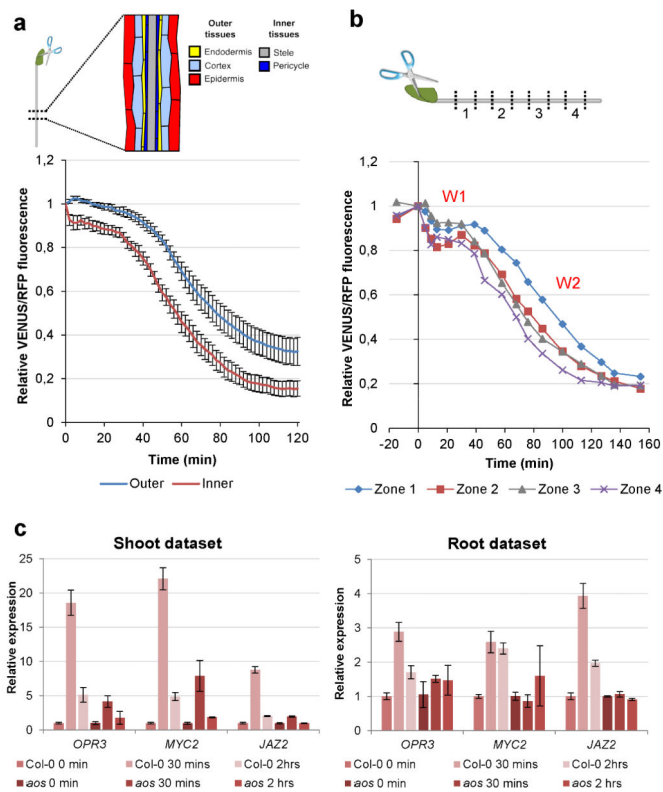


Figure 3. Jas9-VENUS can be used to study long-distance JA signalling in *planta*
(a) Seedlings were wounded by cutting a cotyledon using dissection scissors. Time course quantification of Jas9-VENUS fluorescence, normalised to H2B-RFP fluorescence, in the inner and outer tissues of the root over 120 minutes after wounding. Error bars show the SEM of 13 replicates. **(b)** Time course quantification of Jas9-VENUS fluorescence, normalised to H2B-RFP fluorescence, in the inner tissues at four positions along the root (indicated on the diagram) before and after wounding. **(c)** Shoots and roots of 1-week-old WT or *aos* seedlings were harvested 30 minutes and 2 hours after wounding and the expression of wound-inducible genes were investigated using RT qPCR. The experiment was repeated twice and the results show a representative dataset. Error bars represent the SD of four technical replicates.